



Concept design and neutronics analysis of a heat pipe cooled nuclear reactor with CERMET fuel

Xiaoyu Guo ^a, Yuchuan Guo ^a, Simao Guo ^a, Guanbo Wang ^{a,*}, Zeguang Li ^b, Rundong Li ^a, Zi Wang ^a, Kan Wang ^b

^a Institute of Nuclear Physics and Chemistry, China Academy of Engineering Physics, Mianyang, 621900, Sichuan, China

^b Department of Engineering Physics, Tsinghua University, 100084, Beijing, China

ARTICLE INFO

Keywords:

Heat pipe cooled reactor
CERMET fuel
Megawatt class
Neutronics analysis
RMC

ABSTRACT

Special off-grid power generations require the energy system to be reliable and compact. The heat pipe cooled reactor (HPR) is passively safe and highly modular, and is well suitable for energy demands ranging from a few kW to several MW. This study proposes a compact HPR design in which the ceramic metal composite (CERMET) fuel is used (HPR-CF). The CERMET fuel has advantages such as high temperature resistance and thermal conductivity. The fuel assembly using the CERMET fuel contains 6 heat pipes and fuel blocks with the hexagonal prism shape. The HPR-CF consists of 36 CERMET fuel assemblies containing 216 lithium heat pipes, 12 control drums, 1 safety control rod and peripheral beryllium dioxide reflector, all of which are mounted in a reactor vessel. The Monte Carlo code RMC is used to calculate the neutronics characteristics. The excess reactivity of the HPR-CF reactor is sufficient for operating at high temperature and 3 MWt for over 3000 days. The power distribution and the criticality safety are calculated and discussed. The results show the neutronics availability of the HPR-CF design.

1. Introduction

The energy demand of remote sites such as islands, plateaus, deserts and offshore platforms has been perplexing people living or working there for a long time. It will take much economic and time cost to connect remote sites' grid to the centralized electric grid. For example, China did not power up the whole grid in the Qinghai Tibet Plateau until the end of 2020. Technologies that are useful in off-grid power generations would help to provide more flexible energy applications and to build the decentralized energy generation market. Available technologies include the diesel power, the solar power, the wind power and the nuclear power. The nuclear power is seldom subject to the environmental conditions and the material supply, which makes it more reliable. In addition, the nuclear power is compact and maintains a low carbon emission footprint. Therefore, it is well suitable for cost-insensitive off-grid power generations.

Many small and micro size nuclear power systems have been studied and developed for remote applications, such as the small modular reactors (SMR) using the pressurized water reactor (PWR) (Song et al., 2014; Ingersoll et al., 2014; Kim et al., 2014), the lead-cooled fast reactors (LFR) (Wu et al., 2016) and micro reactors using the heat pipe cooled reactor (HPR) (Arafat and Van Wyk, 2019; Sterbentz et al., 2017). Commonly, the small size PWR and LFR generate more than

10 MW of fission power, and the electric power level of the HPR ranges from a few kW (Gibson et al., 2017) to 20 MW (McClure et al., 2015).

Growing demand for power generation under the 20 MW class has promoted the development of micro reactor designs, in which the HPR technology has been widely used. The HPR uses heat pipes to remove the fission power of the reactor. The heat pipes are usually alkali heat pipes and the reactor core is usually designed as solid reactor. The core transfers the heat to heat pipes by conduction and radiation, and the heat pipes transfer the heat to the energy conversion system by evaporation and condensation of the liquid metal in the pipe. This passive heat transfer feature of the HPR core system makes it get rid of the safety problems caused by valves and motors which will occur in PWR and LFR, and thus the HPR's operation is much easier. Therefore, the HPR is especially suitable for unattended operations at low power level, such as the space nuclear reactors which provides energy for satellites or deep space sensors. The demonstration experiment of the KRUSTY reactor in 2018 (Gibson et al., 2018) showed a successful and practical prototype design of the space HPR.

Another feature of the HPR is that every heat pipe is a single unit with a small feature size, so the reactor can be designed to be modular and easy to expand. By using hundreds of heat pipes, the nuclear

* Corresponding author.

E-mail address: wgb04dep@hotmail.com (G. Wang).

Table 1
Design parameters of three typical megawatt-class HPRs.

Design	MSR	SPR (Design A)	eVinci™
Size of active region	$\phi 48 \times 42$ cm	101.2 cm flat-to-flat 150 cm height	Non-public
Size including reflector	$\phi 88 \times 62$ cm	$\phi 155.7 \times 200$ cm	$\phi 280$ cm
Thermal power	1.2 MWth	5 MWth	15 MWth
Number of heat pipes	129	1134	876
Heat pipe operating temperature	1800 K	948 K	Non-public
Average heat load of every heat pipe	9.3 kWth	4.4 kWth	17.1 kWth (double ended)
Power conversion unit (PCU)	Thermionic	Open-air Brayton	Open-air Brayton, or closed supercritical CO ₂ Brayton
PCU efficiency	> 10%	40.3%	30%

reactor power level could be extended to megawatt class. The megawatt class HPRs can be applied to the off-grid power supply market. Such typical designs include the Martian Surface Reactor (MSR) (Bushman et al., 2011) for space propulsion, the special purpose reactor (SPR) concept (Sterbentz et al., 2017; Guo et al., 2021) designed by Idaho National Laboratory (INL) based on the Los Alamos National Laboratory (LANL)'s Mega-Power concept (McClure, 2015), and the eVinci™ concept designed by Westinghouse (Arafat and Van Wyk, 2019).

The megawatt class HPRs have larger sizes compared with kilowatt class HPRs. However, increasing the size of the reactor core leads to a larger overall size of the nuclear power system, and it could invite troubles in transportation of the nuclear power system. The module dimensions within 2.5 m × 2.5 m (standard container size) in width and height would be better for easy transportation using trucks or rails. The mobile, land-based micro reactor prototype ML-1 (Swartz et al., 2021) developed in the early 1960s was a good practice. Its reactor package's size was 2.44 m × 2.62 m in width and height, and thus could be transported on a military truck or aircraft. It should be mentioned that the outside diameter of the ML-1's reactor vessel is only 0.79 m, leaving the remaining space for radiation shield, thermal management, structural support, instrumentation and control.

Table 1 compares the design parameters of three typical megawatt-class heat pipe reactors. It is obvious that their heat pipes are disparate, due to different working conditions and design limitations of the reactors. The MSR was designed for power supply at planets, and thus the reactor should be compact and launchable. In order to reduce the reactor size, small diameter heat pipes are used. The design goal for SPR and eVinci is to use conventional materials, such as the uranium oxide fuel and the stainless steel, and therefore the design for the heat pipes are conservative with an average heat transfer capability of 5 kWth. Consequently, SPR and eVinci use thousands of heat pipes, which leads to a relatively large diameter of the reactor core. The reactor core diameter of the recent eVinci™ design (Swartz et al., 2021) which generates 15 MWth is 2.8 m. Consequently, the SPR and eVinci™ could not be transported as an integrated package, and extra deployment work is required as stated by McClure (2015). Besides, the reactor decommissioning could also be more difficult.

The reactor size is strongly influenced by the number of heat pipes $N_{\text{heat pipe}}$. The reactor electrical power P_e , power conversion efficiency ϵ , and the average heat transfer power of a single heat pipe $P_{\text{heat pipe}}$ are the factors that influence the number of heat pipes:

$$N_{\text{heat pipe}} = \frac{P_e}{\epsilon P_{\text{heat pipe}}}$$

Improving the power conversion efficiency and increasing the average heat transfer power of a single heat pipe can effectively reduce the number of heat pipes and subsequently the size of the reactor. An effective approach is to raise the operating temperature of the reactor. On the one hand, high temperature heat pipes such as lithium heat pipes could be used, which have higher heat conduction capacity. On the other hand, the power conversion system could be operated at a higher working temperature, which could increase the power conversion efficiency according to the Carnot's theorem. However, high

Table 2
Physical properties of typical materials used in CERMET fuel.

Material	Density (g/cm ³)	Melting point (°C)
Tungsten	19.35	3410
Molybdenum	10.20	2620
UO ₂	10.96	2860
UN	14.4	2847
UC	13.6	2397 ~ 2607

temperature operated nuclear reactor faces many challenges, of which the most difficult problem is the fuel assembly. Its nuclear fuel assembly could suffer from not only the high operating temperature but also more tough design basis accident and more fission gas release after long-term operation.

The ceramic–metal (CERMET) fuel is a viable solution to overcome these difficulties. The CERMET fuel is a type of dispersion fuel (Burkes et al., 2007). The matrix material of the CERMET fuel is refractory alloy such as the tungsten alloy or the molybdenum alloy. Nuclear fuel kernels made up of UOX, UN or UC are dispersed in the refractory alloy. Table 2 lists the density and melting point properties of those materials. It is obviously found that all the melting points are more than 2000 °C, and therefore they are temperature resistant. The CERMET fuel was developed firstly as the fuel for nuclear thermal propulsion (NTP) system. The NTP systems are typically characterized by very high temperature exhaust gas ($T_{ex} \approx 2277 \sim 2627$ °C) (Burns and Johnson, 2020; Stewart, 2015). The CERMET fuel has proven to be capable of tolerating the effects of numerous temperature cycles through numerous testing and studies (Haertling and Hanrahan, 2007). The cladding of the CERMET fuel may deform but not be harmed during thermal cycling. Moreover, the containment of fission products is improved with the CERMET fuel. Thus, the CERMET fuel is appropriate for mobile small reactors that operate in frequent startup and shutdown modes at high temperatures.

This study proposes a compact HPR design using the CERMET fuel. The CERMET fuel uses the tungsten alloy as the matrix and the uranium carbide as the fuel kernel, which has been used in nuclear thermal propulsion (NTP) reactors. Section 2 provides the HPR-CF design, in which the reactor core is compact based on the thermal properties of the W-UC CERMET fuel. Section 3 investigates the neutronics characteristics of the HPR-CF, including the excess reactivity, the burnup performance, the power distribution and so on. More discussions are presented in Section 4.

2. Design of the HPR-CF

The design of the HPR-CF begins with a goal that the system should be compact and extensible, and with a criteria that the power level should be megawatt class. To reach the goal, the heat transfer capability of every heat pipe should be high enough to decrease the total number of the heat pipes and thus to reduce their volume. Therefore, it is decided to use high temperature lithium heat pipe in the HPR-CF design. Accordingly, the CERMET fuel is chosen to meet the operating temperature requirements. However, the CERMET fuel is much heavier

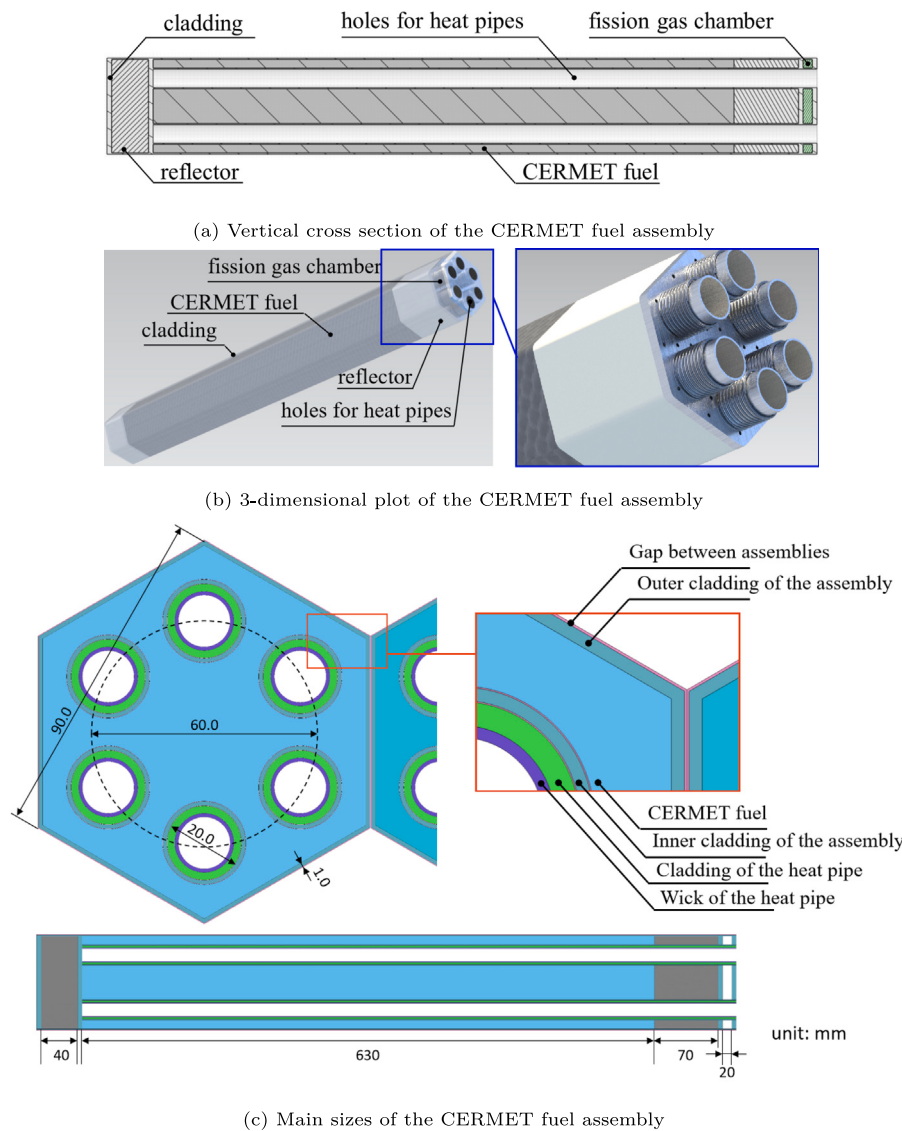


Fig. 1. Structure of the CERMET fuel.

than the common nuclear fuels, which increases the manufacturing difficulty. Thus, the heat pipes and the CERMET fuel are made into assemblies as follows for easy-fabrication.

2.1. Determination of the neutron spectrum

The neutron spectrum of the HPR-CF is determined to be fast spectrum. Many HPR designs proposed and published recently, such as the MHPR (Chai et al., 2022), HPTWR (Ma and Hu, 2022), and MHR (Li et al., 2022), chose the thermal neutron spectrum design. The thermal reactors can significantly improve the utilization of ^{235}U , but will also somehow increase the reactor size because additional moderator elements are required in the active region to slow down high-energy fission neutrons. Besides, since many high-performance moderator materials, such as metal hydrides, have low melting points and lower working temperature due to decomposition problems, the operation temperature is usually limited below 1000 K.

The design of HPR-CF is required to develop a reactor with very compact size, so that the reactor core could be packed into a truck container. A fast reactor design can significantly reduce the reactor dimensions. Besides, the power conversion efficiency is required to be larger than 30% with an open-air Brayton cycle, which caused the

reactor working at very high temperature beyond the range for most high-performance moderator materials. Therefore, this study chose to use fast spectrum and high enriched uranium in HPR-CF. Some HPR designs published in recent years also used fast spectrum and high enriched uranium, such as the HPCR (Zhang et al., 2020) and NUSTER (Guo et al., 2023). In addition, the CERMET fuel is also more compatible with fast reactors.

2.2. Design of the HPR-CF CERMET fuel assembly

The CERMET fuel is a type of dispersion fuel, in which the fuel is ceramic particles and the matrix is metals or alloys. In the HPR-CF design, the ceramic fuel is the uranium carbide (the uranium nitride is an alternative option) and the alloy matrix is the tungsten alloy. There are several advantages of the W-UC CERMET fuel:

1. High melting point. The melting point of the tungsten metal is around 3400 °C, the highest melting point of any metal. The melting point of most tungsten alloys is more than 2000 °C, which is much larger than the reactor operating temperature. The melting point of the UC is also more than 2000 °C (Bobkov et al., 2008).

2. High thermal conductivity. The thermal conductivity of the tungsten metal is around $170 \text{ W} \cdot \text{m}^{-1} \cdot \text{K}^{-1}$, and the thermal conductivity of the uranium carbide is around $25 \text{ W} \cdot \text{m}^{-1} \cdot \text{K}^{-1}$ (Bobkov et al., 2008). Although little information of the W-UC is available, the thermal conductivity of similar CERMET fuels such as the W-UN fuel is more than $30 \text{ W} \cdot \text{m}^{-1} \cdot \text{K}^{-1}$ (Webb and Charit, 2012).
3. High radiation shielding capability. The atomic number of the tungsten is 74 and its atomic mass is 183.84 mu. Therefore, the tungsten element in the W-UC fuel has a good radiation performance on γ rays.

Motivated by the properties above and the fabrication of the CERMET fuel used in NTP reactors (Brengele et al., 1993), the CERMET fuel assembly is designed as a hexagonal prism that contains six heat pipes. Figs. 1(a) and 1(b) depicts the structure of the HPR-CF CERMET fuel assembly. A fuel assembly consists of several CERMET fuel blocks in the active region, two reflectors made of BeO on the top and bottom of the assembly, a small fission gas chamber on the top, the fuel cladding which is made of tungsten and covers the fuel and reflectors, and six heat pipes. The CERMET fuel blocks and the fuel cladding are weld together for a better mechanical performance. The pitch off the fuel assembly is 9 cm, which was determined by the design of the heat pipe exchanger that will be shown in another study completed by other researchers. The heat pipes are inserted into the assembly holes. The size of the gap between the fuel cladding and the heat pipes is 0.1 mm, which could be further decreased if the linearity of the heat pipes and the holes could be improved. Fig. 1(c) provides detailed dimensions of the CERMET fuel assembly.

The packing fraction of the W-UC CERMET fuel and the ^{235}U enrichment are dependent both on the sintering technology which is under development and the requirement to reach criticality. In the current design, the UC kernel radius is 150 μm which size was suggested by the nuclear fuel processing plant. The structural design of the nuclear power system requires the HPR-CF core to be light-weighted as much as possible. It should be noted that increasing the packing fraction of the fuel will help increase the uranium density, which can reduce the size of the active region. Besides, since the density of tungsten is pretty high, the weight of the fuel pellets can also be reduced. The packing fraction of the fuel was determined to be 40%, which is a relatively large value that can be achieved by the existing equipments and processes of the nuclear fuel processing plant.

Common working fluids of the heat pipes include the potassium, sodium and lithium. In these three available options, the lithium heat pipe operates at the highest temperature and has the largest heat transfer limit. Therefore, the HPR-CF uses the lithium heat pipe and the normal operating temperature is 1050 °C. Considering the power peak factor, the single heat pipe failure accident and the difference between the theoretical and the practical value of the heat transfer limit, the average heat transport of each heat pipe is around 14 kWth. Consequently, the average rated power of each assembly is 84 kWth.

The assembly design parameters are summarized in Table 3. The flat-to-flat size is 90 mm, which is compatible with the heat pipe exchanger dimensions that will be discussed in the paper of the system design study. It is noted that the fission gas chamber height is small. Although little data is available for the long-term irradiation performance of the CERMET fuel, especially the containment capability of the fission gases, dispersion fuels such as the well-known TRISO fuel (Powers and Wirth, 2010) and the $\text{U}_3\text{O}_8\text{-Al}$ plate type fuel (Bergeron, 2013) used by HFIR do not even involve a fission gas containing space. The fission gas chamber is designed to ensure the safety of the current design, and may be deleted after CERMET fuel irradiation tests.

Table 3
Main parameters of the CERMET fuel assembly of the HPR-CF design.

Parameter	Value	Unit
Flat-to-flat size	90	mm
Assembly height	780	mm
CERMET fuel height	630	mm
Top reflector height	70	mm
Bottom reflector height	40	mm
Fission gas chamber height	20	mm
Cladding thickness	1	mm
Heat pipe hole length	730	mm
Heat pipe diameter	20	mm
Heat pipe length	2500	mm
Heat pipe evaporation length	700	mm
Heat pipe condenser length	800	mm
Operating temperature	1050	°C
Cladding material	Tungsten	-
Reflector material	Beryllium dioxide	-
Heat pipe cladding material	TZM alloy	-
Gap material	Helium	-
Heat pipe working medium	Lithium	-
CERMET fuel material	W-UC	-
Dispersion fuel packing fraction	40%	-
Fuel kernel radius	150	μm
^{235}U enrichment	65%, 75%, 85%	-
Average ^{235}U weight per assembly	10.0	kg
U weight per assembly	13.3	kg
Assembly weight	54.1	kg

2.3. Materials of the HPR-CF reactor core

Besides the fuel pellets, it is also important to choose the materials for other components including the reflector, the heat pipe cladding wall, and the reactor core container.

Common materials for usage as reflectors include Be, BeO, MgO, Al_2O_3 , etc. Among these materials, the metal Beryllium has the best performance. However, the melting point of Beryllium is only 1287 °C, which is very close to the operating temperature of HPR-CF. The second best moderator is BeO with the melting point of 2530 °C, and thus was chosen as the reflector material. Usage of MgO or Al_2O_3 is much cheaper but will increase the reactor size and weight.

The TZM alloy is used as the heat pipe cladding wall because of its excellent high-temperature mechanical properties, such as its high strength and toughness at high temperatures which make it suitable for use as the heat transfer boundary between the nuclear reactor core and the heat exchanger. However, the production of TZM alloy is still a difficult issue. Therefore, the common Mo-Re alloy is also an option. It is noted that the TZM alloy is also a type of molybdenum-based alloy, and thus the change between TZM alloy and Mo-Re alloy does not affect the neutronics characteristics obviously.

The Mo-14Re alloy also offers good high-temperature properties and is easier for production compared to the TZM alloy. What is important is that the mechanical data of the Mo-14Re after nuclear reactor irradiation could be obtained by our experiments on China Mianyang Research Reactor (CMRR). Therefore, the usage of the Mo-14Re alloy is more mature and is thus selected as the container material.

2.4. Layout of the HPR-CF reactor core

Based on the CERMET fuel assembly, the HPR-CF is designed to be compact and simple. The layout of the HPR-CF is depicted in Fig. 2, and parameters of the reactor components are listed in Table 4.

The HPR-CF uses different ^{235}U enrichment (65%, 75% or 85%) in assemblies at different positions, respectively, in order to reduce the radial power peak factor. With uniform fuel enrichment, the radial power peak factor was calculated to be 1.267 with all control drums open, and the reactor core power peak factor will be larger than 1.6. However, if the 36 CERMET fuel assemblies in 3 circles use fuels of different ^{235}U enrichment: 65% in the center circle, 75% in the middle

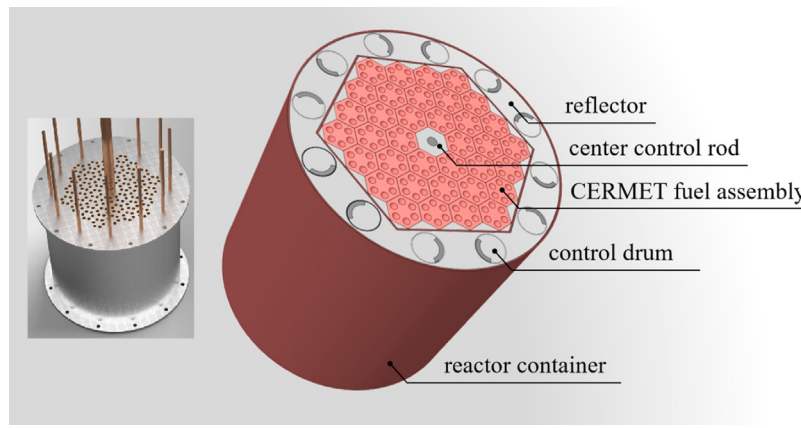


Fig. 2. Layout of the HPR-CF.

Table 4
Components' parameters of the HPR-CF.

Parameters	Value	Unit
Number of fuel assemblies	36	–
Pitch of fuel assembly	90	mm
Gap size between fuel assemblies	0.2	mm
Number of heat pipes	216	–
Number of control rod assemblies	1	–
Materials of control rod assemblies	Enriched B ₄ C with 92% ¹⁰ B and 8% ¹¹ B (absorber), W (cladding), BeO (reflector)	–
Number of control drums	12	–
Materials of control drums	Enriched B ₄ C with 92% ¹⁰ B and 8% ¹¹ B (absorber), W (cladding), BeO (reflector)	–
Number of radial reflectors	6	–
Material of radial reflectors	BeO	–
Material of reactor container	Mo-14Re	–
Reactor height	< 800	mm
Reactor diameter	< 850	mm
Reactor weight	3.1	t

circle and 85% in the outer circle, the radial power peak factor will be reduced to below 1.1, as shown in Section 3. As a result, the uranium density is around 4.9 g/cm³ accordingly, and every CERMET fuel assembly contains around 13.3 kg U and 10.0 kg ²³⁵U in average.

Outside of the fuel assemblies are radial reflectors, in which 12 control drums are located for reactivity control. At the center of the reactor core is a control rod assembly as the safety rod for emergency shutdown. All of the above components are assembled into a container made of the Mo-14Re alloy, and the container will be put into a reactor vessel fulfilled with helium.

The operation temperature of the heat pipes is designed to be 1050 °C. The designed thermal power of the HPR-CF is 3.0 MWt, and the designed electric power of the HPR-CF is 1.0 MWe, which indicates that the energy conversion efficiency of the secondary loop is 33.3%. The PCU uses an open air Brayton cycle in conjunction with a closed organic working medium Rankine cycle, with a design energy conversion efficiency of 35%. This is a conservative estimation compared with the SPR design parameters in which the operating temperature of the heat pipes is 675 °C and the energy conversion efficiency of the secondary loop is over 40%.

3. Neutronics analysis of the HPR-CF

The neutronics characteristics including the excess reactivity, the power distribution, the criticality safety, etc. are basic and key factors affecting the performance of the reactor. These characteristics are analyzed using the Monte Carlo code RMC (Wang et al., 2015), a neutron-photon-electron transport code developed by the Reactor Engineering Analysis Lab (REAL) of Tsinghua University. The accuracy of the RMC code has been validated by criticality benchmarking (Zheng

et al., 2020). Most importantly, the RMC code is capable of modeling the dispersion fuel in a more accurate way (Liu et al., 2015), as well as calculating the burnup process of the dispersion fuel (Liu et al., 2016a), which is essential for this study. Besides, the on-the-fly (OTF) temperature-dependent cross-sections treatment function (Liu et al., 2016b, 2018) enables the simulation of the HPR-CF operating at high temperature.

The HPR-CF model built by RMC is shown in Fig. 3, in which the fuel particles are modeled implicitly by the stochastic media analysis capability of RMC based on the Chord Length Sampling method (Liu et al., 2015). All the simulations below was carried out using 200 source convergence cycles and 400 tally cycles with 100,000 neutrons simulated per cycle. With this configuration, the statistical uncertainty of k_{eff} is around 0.0001, which is enough for a good results statistic because the k_{eff} changes caused by burnup, temperature feedback, control drums' rotation, et al. in this study is of the order of 0.01 which will be shown in the next sections, much larger than the statistical uncertainty. The calculation speed is around 900 neutrons per second per thread, and the memory footprint is about 300 Mb per thread in k-eigenvalue calculations.

3.1. Excess reactivity

The reactivity of the reactor core is controlled by rotating the control drums. When the absorbers in the control drums are facing outside of the core as shown in Fig. 4(a), and the reactor is at the room temperature, the neutron multiplication capability of the reactor core reaches the highest, which could provide excess reactivity for temperature feedback and burnup. The excess reactivity is 0.04164 $\Delta k/k$ by calculation. The maximum reactivity control capability of the drums is

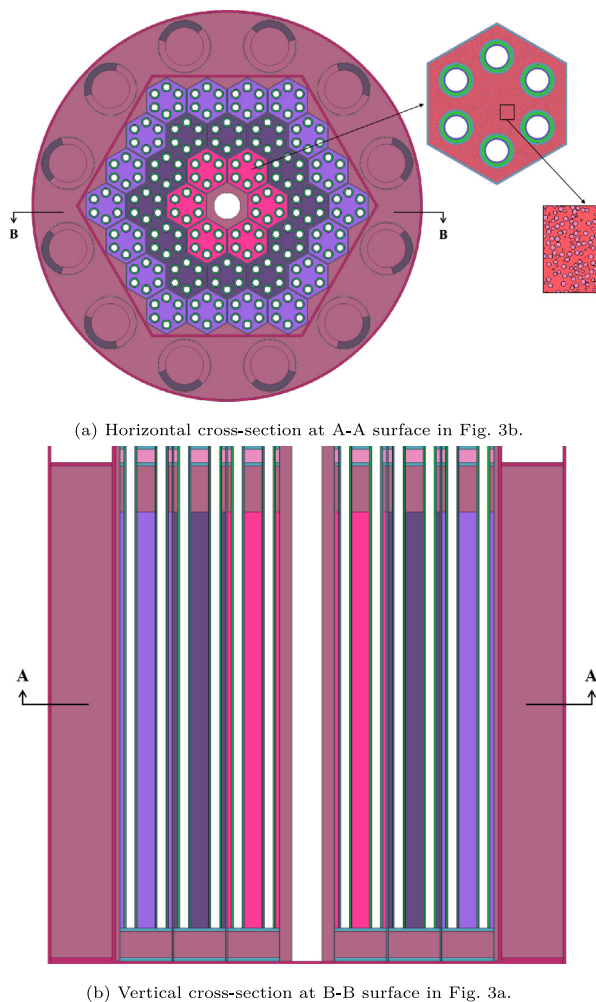


Fig. 3. HPR-CF model built and plotted by the RMC code.

reached when the absorbers are facing toward the core centerline, as shown in Fig. 4(b).

Fig. 5 shows two control drums' integral reactivity worth curves at hot full power and cold zero power, respectively. It is found that the two curves are very similar, in which the curve at hot full power is slightly lower than the curve at cold zero power. The reactivity control capability of the control drums is $0.05051 \Delta k/k$ at hot full power and $0.05127 \Delta k/k$ at cold zero power. Therefore, with all control drums closed and the reactor shutdown, the subcritical margin is $0.00963 \Delta k/k$, which is close to $1\% \Delta k/k$, the cold state shutdown margin of some small-size research reactors such as the China Advanced Research Reactor (CARR) and the China Mianyang Research Reactor (CMRR). This indicates that the control drum system may be used as an independent shutdown system. Besides, the safety rod in the center of the reactor yields a control worth of $0.05339 \Delta k/k$, which enables it as a second independent shutdown system.

A burnup calculation was carried out to obtain the reactivity loss caused by fissile nuclides' consumption during reactor operation. Every fuel assembly was divided into 10 zones axially as Fig. 6 shows, and there are 360 depletion zones in total. The reactivity and burnup against the core life is shown in Fig. 7. After 3000 effective full power days' operation, the reactivity loss due to the burnup is $0.01779 \Delta k/k$, and the total burnup is around 20 Gwd/tHM. The evolution of ^{235}U , ^{238}U , ^{239}Pu and ^{241}Pu is shown in Fig. 8. It is found that the consumption of ^{235}U after 3000 days' full power operation is around 12 kg, only 3.3% of its initial inventory. The burnup depth is significantly low

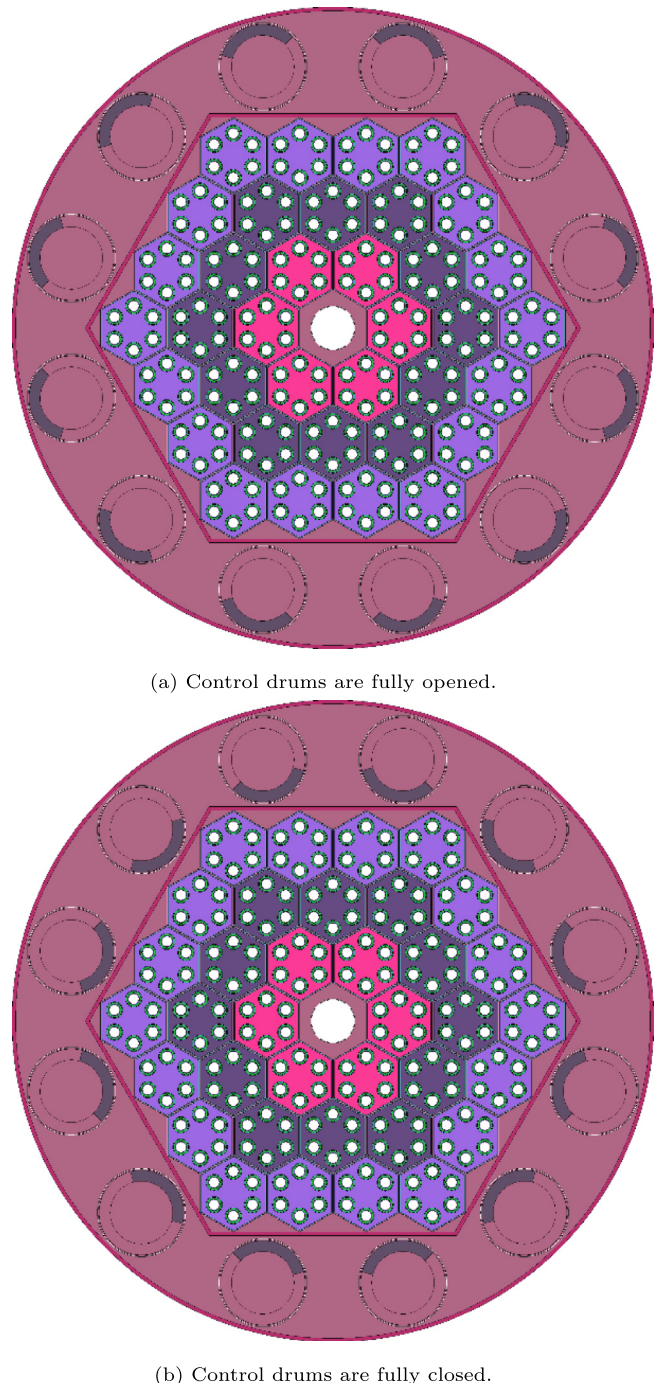


Fig. 4. States of the control drums at different conditions.

especially compared with those reactors moderated and cooled by light water. The reason is that the HPR-CF is a fast neutron reactor and is designed without refueling. The burnup is also low for some small-size fast reactors, such as the China Experimental Fast Reactor(CEFR) which yields an average discharge burnup of only 4.62%. In addition, many heat pipe cooled reactors also have low burnup depth. For example, the burnup of SAFE-300 is 0.92 at.% over a ten-year period (Amiri and Poston, 2002), the burnup of eVinci is less than 10 Mwd/kgU with fuel enrichment between 5% and 19.75% (Subki, 2020), and the maximum fuel assembly burnup of a recent heat pipe reactor design proposed by Sun et al. (2018) is 7.2 Mwd/kgU with the fuel enrichment of 70% over a 14 year period. As Allaf et al. (2023) stated in their study, the

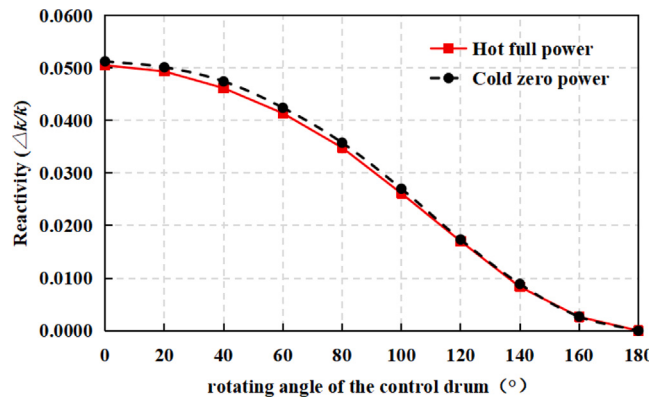


Fig. 5. Integral reactivity worth curve of the control drums against the rotating angle.

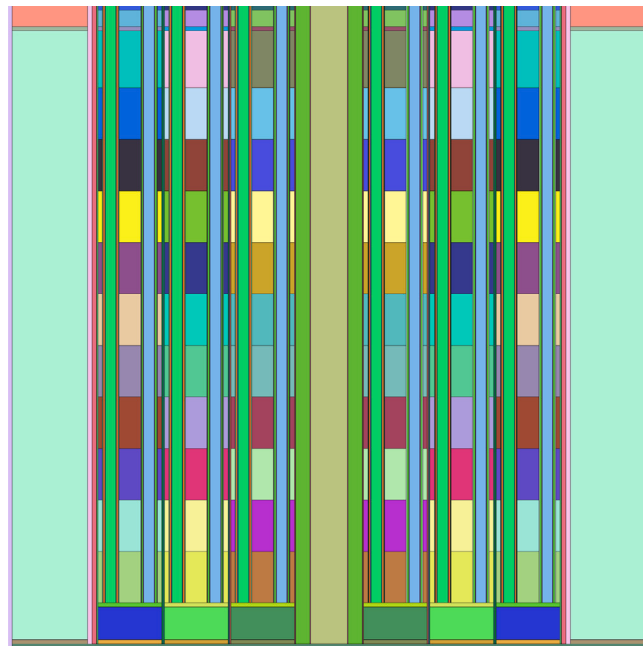


Fig. 6. Depletion zone.

HALEU micro reactors cooled by heat pipes does not permit for high burnup, which case is similar for most HPRs.

The temperature feedback effect is also evaluated. Fig. 9 presents the Doppler broadening effect, in which the temperature feedback is obviously negative. Considering both the Doppler broadening effect and the thermal expansion effect, the results are listed in Table 5. The temperature feedback coefficient was calculated using Eq. (1).

$$K_T = \frac{k_{\text{eff},1500 \text{ K}} - k_{\text{eff},300 \text{ K}}}{1500 \text{ K} - 300 \text{ K}} \quad (1)$$

The Doppler broadening effect was evaluated using the on-the-fly Doppler broadening function of RMC, in which the neutron cross-sections were broadened from 300 K to 1500 K based on the Gauss-Hermite integration. The thermal expansion effect was evaluated by changing the fuel pellets' and the reflectors' density and dimension. In this study, the coefficient of linear thermal expansion (CTE) of tungsten is $4.4 \times 10^{-6} \text{ K}^{-1}$, the CTE of UC is $10.98 \times 10^{-6} \text{ K}^{-1}$, and the CTE of BeO is $8.3 \times 10^{-6} \text{ K}^{-1}$. The thermal expansion was supposed to be isotropic, and the density was reduced so that the mass of the pellets and the reflectors

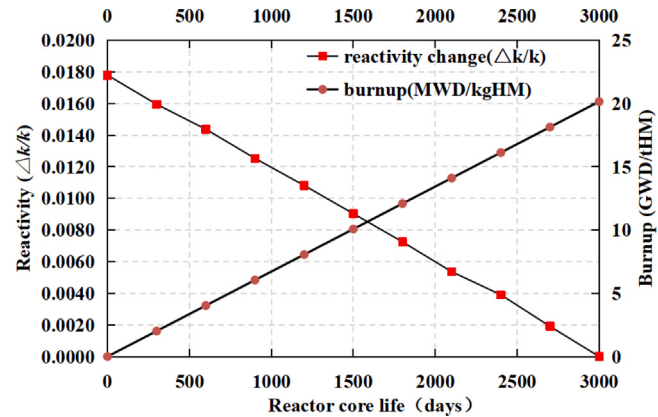


Fig. 7. Reactivity and burnup for the HPR-CF reactor core operating at 3 MWt for over 3000 days.

Table 5
Temperature feedback of the HPR-CF reactor core.

Temperature	300 K	1500 K
k_{eff}	1.04345 ± 0.00010	1.03324 ± 0.00011
Temperature feedback coefficient	$-7.89478 \times 10^{-6} \text{ K}^{-1}$	

Table 6
 k_{eff} change with different shielding thickness.

Radial thickness	Axial thickness	k_{eff}
0.0 cm	0.0 cm	1.04345 ± 0.00011
0.5 cm	0.5 cm	1.04420 ± 0.00010
1.0 cm	1.0 cm	1.04523 ± 0.00011
2.0 cm	2.0 cm	1.04610 ± 0.00010
3.0 cm	3.0 cm	1.04604 ± 0.00010
4.0 cm	4.0 cm	1.04631 ± 0.00010

was kept constant. It is found that the reactivity loss due to the temperature feedback is $0.00947 \Delta k/k$. Therefore, the total reactivity loss due to burnup and temperature feedback is $0.02726 \Delta k/k$, less than the excess reactivity.

It is also noted from previous studies (Guo et al., 2021; Yan et al., 2020) that the shielding structure outside of the core container affects the neutronic results by changing the neutron leakage effect which is strong in microreactors. Although detailed shielding design is not decided yet, a simple neutron shielding structure was used herein to investigate this effect on the neutron effective multiplication factor which is supposed to increase with thicker shield. The reactor core is surrounded radially and axially by Lithium hydride which is a type of excellent reflector, that is, the deep blue region shown in Fig. 10. Table 6 presents the k_{eff} results. Obviously, the k_{eff} reaches steady when the shield thickness is larger than 2 cm, and the maximum reactivity is $0.04426 \Delta k/k$, which may also be controlled by the control drums and the safety rod.

3.2. Neutron flux and fission power distribution

The HPR-CF was designed as a fast spectrum reactor to enable the reactor to operate for 3000 full power days without refueling. The neutron flux distribution is shown in Fig. 11. With all control drums open, the neutron flux near the outside edge of the reactor is low, especially at the absorber regions. The neutron flux at the active region is typically larger than $4.5 \times 10^{13} \text{ n/cm}^2 \text{s}$.

Fig. 12 depicts the neutron flux spectra in region of the HPR-CF assemblies and reflector at beginning-of-life (BOL) and end-of-life (EOL). Obviously, the burnup process has little effect on the neutron

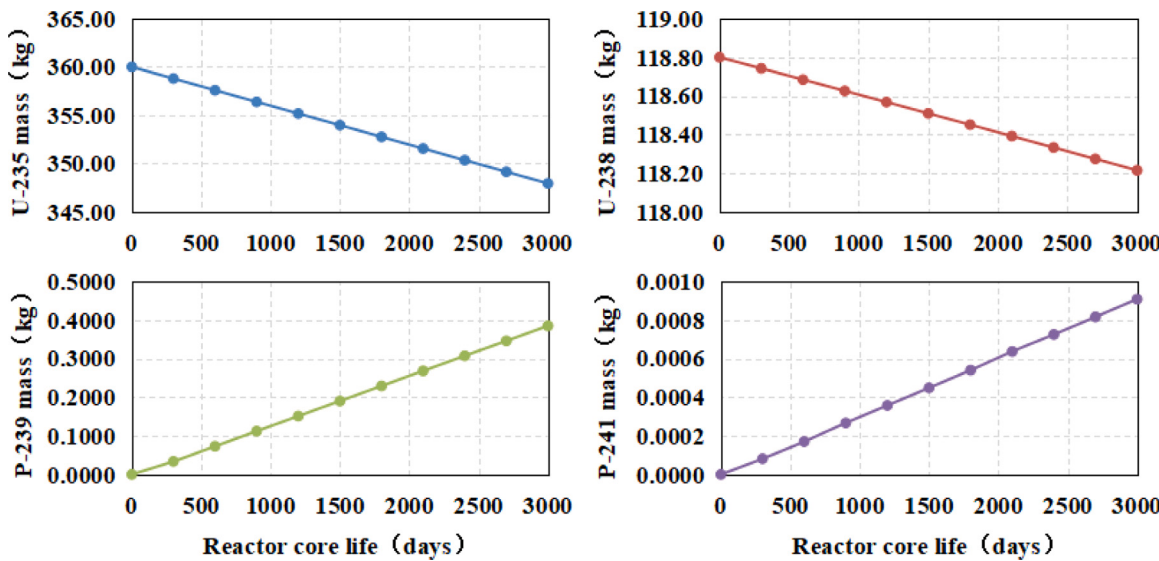


Fig. 8. Evolution of U-235, U-238, Pu-239 and Pu-241 during burnup over 3000 days.

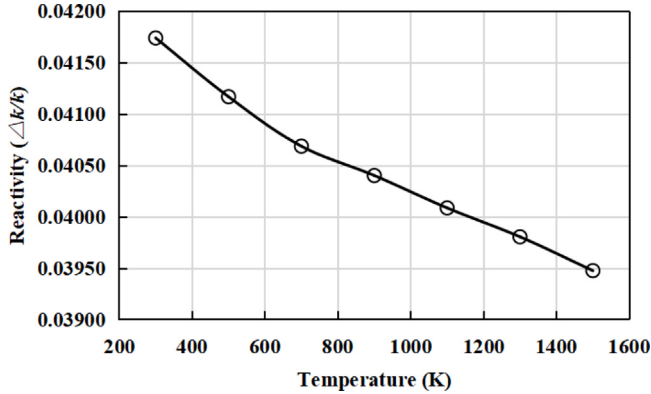


Fig. 9. Reactivity variation with core temperature as a result of the Doppler broadening effect.

Table 7
Neutron fraction in different energy regions.

Neutron energy	Assemblies	Reflector
Thermal neutron	0.03%	2.48%
< 0.625 eV		
Epithermal neutron	29.55%	65.63%
0.625 ~ 0.1 MeV		
Fast neutron	70.42%	31.89%
> 0.1 MeV		

flux spectra. The neutron flux spectra is harder in the assemblies region than in the reflector region. As listed in Table 7, the fast neutrons account for over 70 percent of all the neutrons in the assemblies region while they are less than 32 percent in the reflector region.

It is noted that the enrichment of ^{235}U is higher in the fuels of the outer circle than the inner circle. Consequently, the radial power peak factor could be reduced. Fig. 13 shows the normalized distribution of the assembly power (by solving the k-eigenvalue problem) of different states. With the rotation of the control drums from 0° to 180° , the relative power of the assemblies at the edge of the active region is lowered and the relative power of the assemblies at the central region is increased. Fig. 14 shows the normalized power distribution in the axial direction. The rotation of the control drums has little affect on

the axial power distribution because the material composition in the axial direction does not change with the rotation. It is observed that the power profile is almost symmetry, as a result of the top and bottom reflectors of different sizes. The power peak factors are summarized in Table 8. All the power peak factors are less than 1.5.

Fig. 15 depicts the hyperfine axial power distribution of all the assemblies. Note that the power distribution inside every assembly is significantly non-uniform, especially for the inner assemblies. This phenomena occurs due to the space self-shielding effect since the size of the CERMET fuel is larger compared with common fuel rods or annular fuels. Consequently, the inhomogeneity will lead to the unbalanced thermal load for the six heat pipes inside one assembly, and its affect on the heat pipes' safety characteristics needs to be studied further.

With the operation of the HPR-CF reactor, the consumption of the fissile nuclides always lead to a re-distribution of the radial power. However, because the total burnup of the HPR-CF is around 20 GWD/tHM even after 3000 days' full power operation, there is only a little change in the radial power distribution. As shown in Fig. 16, the radial power peak factor is 1.029 at EOL, only 0.57% less than that at BOL.

3.3. Criticality safety and kinetic parameters

During the operation of the micro nuclear energy system for off-grid power generations, criticality safety issues may occur, among which the flooding accident is the typical one. This study makes the assumption that all the gaps of the reactor core such as the gaps between heat pipes and fuel claddings will be filled by water in the flooding accident, and the outside of the reactor core is also filled by water. Under this condition, the reactor core should be sub-critical if the reactivity control system works. Table 9 lists the neutron effective multiplication factor of the reactor core under cold conditions with no burnup. It is found that the reactor core meets the critical safety even without the center control rod.

The kinetic parameters of the HPR-CF reactor core are also calculated. The parameters of the delayed neutron are listed in Table 10. The prompt neutron lifetime is $0.408 \mu\text{s}$, and thus the average neutron lifetime of the HPR-CF reactor core is 0.075 s .

4. Discussion and conclusions

Among the candidates for the off-grid power generations, the nuclear energy is more stable and sustainable than the diesel power, and

Table 8

Power peak factor of the HPR-CF reactor core.

Reactor core state	Radial power peak factor	Axial power peak factor	Reactor core power peak factor
Control drums are fully opened	1.035		1.310
Criticality	1.102	1.266	1.395
Control drums are fully closed	1.180		1.494

Table 9

Criticality safety characteristics of the HPR-CF reactor core.

Reactor core state	k_{eff}
Control drums are closed, control rod is withdrawn	0.99355 ± 0.00011
Control drums are closed, control rod is inserted	0.93506 ± 0.00010

Table 10

Kinetic parameters of the HPR-CF reactor core.

Delayed neutron family	Delay constant (s^{-1})	Average lifetime (s)	Effective fraction
1	0.013340	74.96	0.000236
2	0.032706	30.58	0.001229
3	0.120860	8.27	0.001181
4	0.303580	3.29	0.002655
5	0.852900	1.17	0.001113
6	2.863800	0.35	0.000464

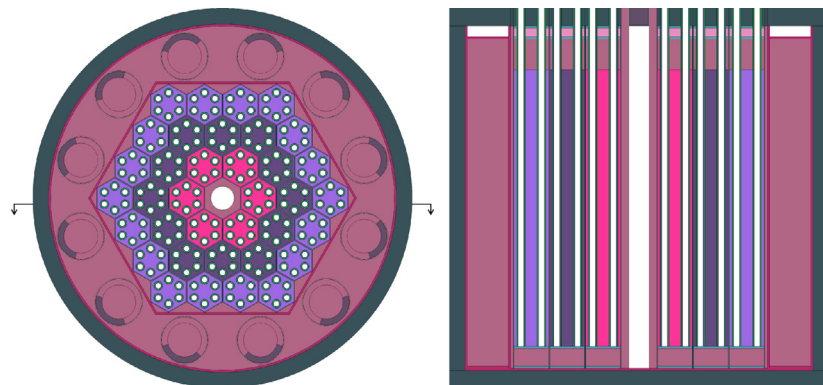


Fig. 10. Reactor layout with simple shielding structure.

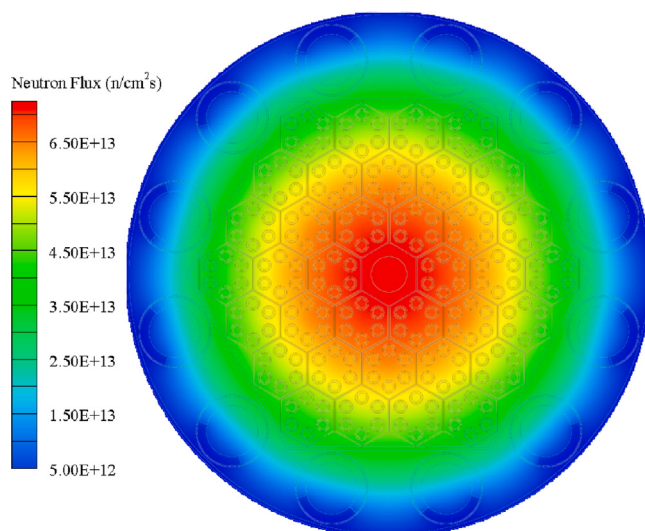


Fig. 11. Neutron flux radial distribution with all control drums open.

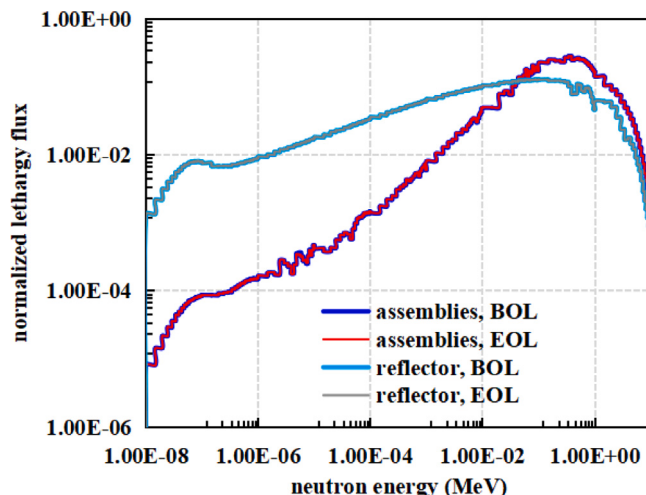


Fig. 12. Neutron flux spectra at BOL and EOL.

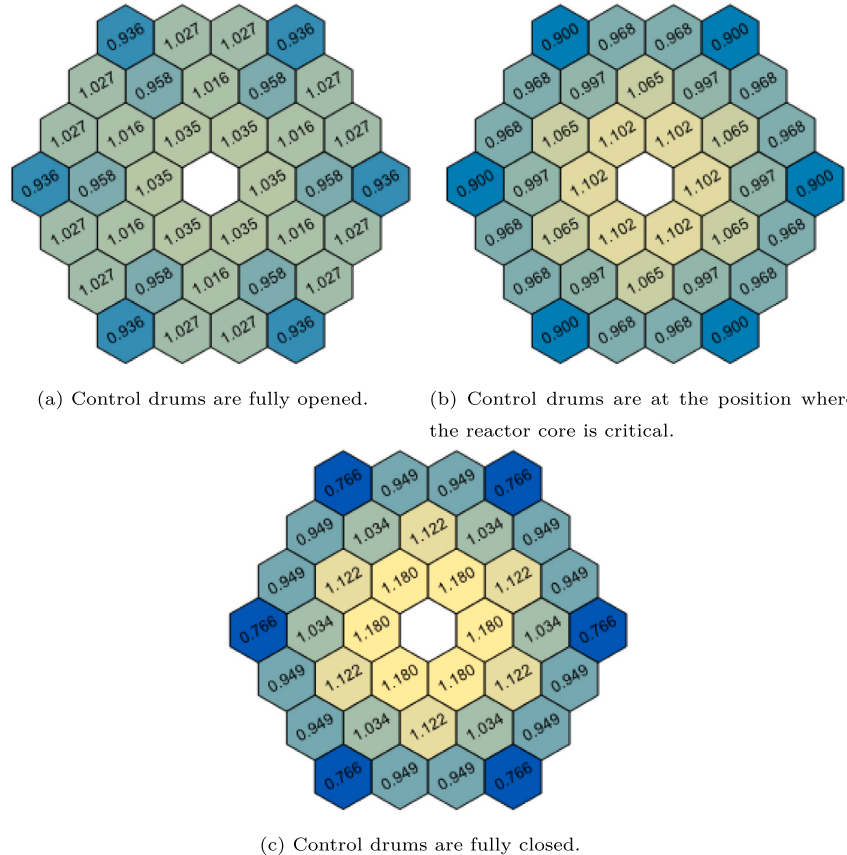


Fig. 13. Normalized power distribution of all the assemblies.

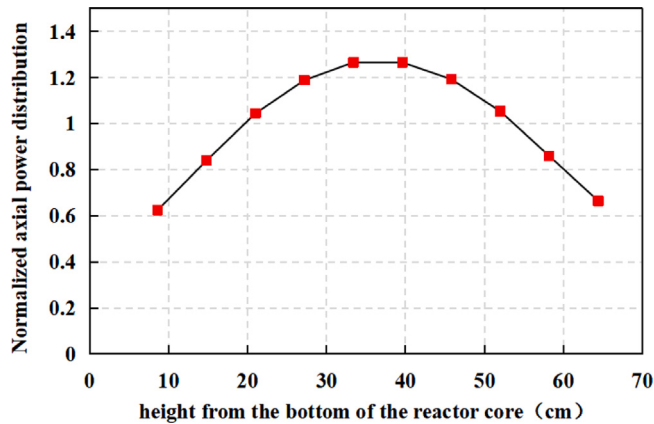


Fig. 14. Normalized axial power distribution.

more compact and flexible than the solar and wind power. To meet the demand for easy transportation and decommissioning, it is better to reduce the size of the nuclear power system. A lithium heat pipe cooled nuclear reactor design with CERMET fuel is proposed in this study. Because of the high temperature and high thermal conductivity

characteristics, the fuel assembly of the HPR-CF reactor core is compact, which contributes to a small size design of the HPR-CF reactor core operating at 3 MWt for over 3000 days.

The neutronics characteristics of the HPR-CF reactor core is calculated based on the RMC code's advanced functions (dispersion fuel burnup simulation and the OTF temperature-dependent cross-section treatment), and the results are summarized as follows:

- The excess reactivity is adequate so that the HPR-CF reactor could operate at high temperature and full power for over 3000 days.
- The radial and axial peak power factor of the HPR-CF reactor core are within 1.2 and 1.3, respectively, which could reduce the thermal load imbalance of the heat pipes and improve the safety.
- The criticality safety could be maintained at the flooding accident. Even without the safety control rod, the control drums could still provide sufficient protection capability.

Generally, the HPR-CF reactor core design is compact and effective. The power tilt phenomena occurred within every CERMET fuel assembly, as well as the optimization work for a better thermal-mechanical performance will be investigated in future studies.

CRediT authorship contribution statement

Xiaoyu Guo: Conceptualization, Modeling, Formal analysis, Writing – original draft and revising. **Yuchuan Guo:** Modeling, Formal analysis. **Simao Guo:** Conceptualization, Formal analysis. **Guanbo Wang:**

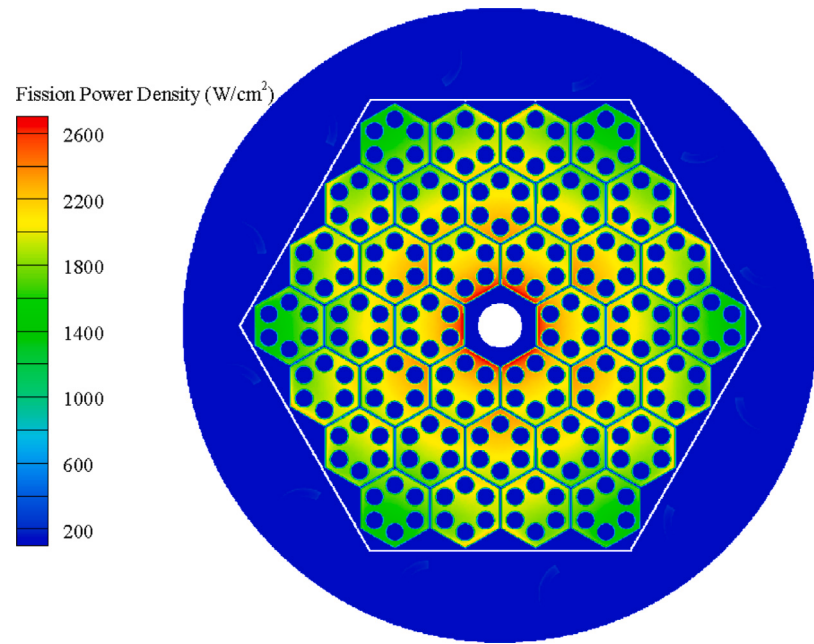


Fig. 15. Hyperfine radial power distribution of all the assemblies.

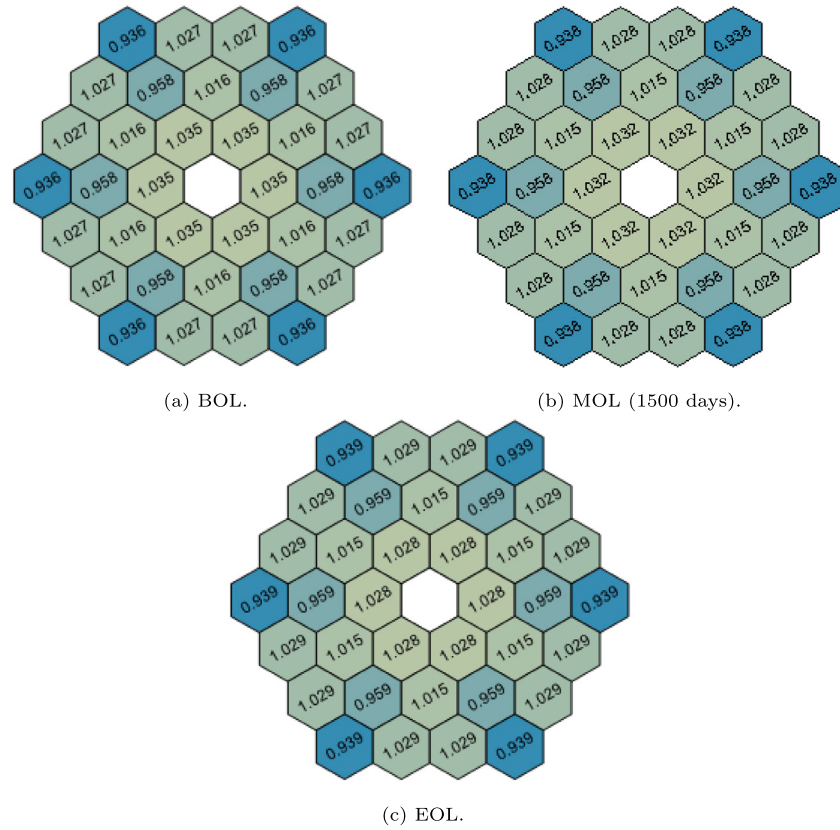


Fig. 16. Change of the normalized radial power distribution with the burnup.

Conceptualization, Supervision, Writing – review & editing, Resources. **Zeguang Li:** Software, Methodology. **Rundong Li:** Supervision, Funding acquisition. **Zi Wang:** Modeling. **Kan Wang:** Funding acquisition.

Declaration of competing interest

The authors declare that they have no known competing financial interests or personal relationships that could have appeared to influence the work reported in this paper.

Data availability

Data will be made available on request.

Acknowledgment

This study was supported by the National Key Research and Development Project of China (Grant No.: 2020YFB1901700).

References

- Allaf, M., Okamoto, K., Erkan, N., 2023. Conceptualization of the micro research reactor cooled by heat pipes (MRR-HP), part-I: Neutronics analyses. *J. Nucl. Sci. Technol.* 60, 299–319.
- Amiri, B.W., Poston, D.I., 2002. Burnup calculations for the HOMER-15 and SAFE-300 reactors. In: AIP Conference Proceedings, vol. 608. American Institute of Physics, pp. 681–685.
- Arafat, Y., Van Wyk, J., 2019. Evinci micro reactor. *Nucl. Plant J.* 37, 34–36.
- Bergeron, A., 2013. Review of the Oak Ridge National Laboratory (ORNL) Neutronic Calculations Regarding the Conversion of the High Flux Isotope Reactor (HFIR) to the Use of Low Enriched Uranium (LEU) Fuel. Tech. Rep., Argonne National Lab. (ANL), Argonne, IL (United States).
- Bobkov, V., Fokin, L., Petrov, E., Popov, V., Rumiantsev, V., Savvatimsky, A., 2008. Thermophysical properties of materials for nuclear engineering: A tutorial and collection of data. IAEA, Vienna.
- Brengle, R., Harty, R., Bhattacharyya, S., 1993. The promise and challenges of cermet fueled nuclear thermal propulsion reactors. In: 29th Joint Propulsion Conference and Exhibit. p. 2111.
- Burkes, D.E., Wachs, D.M., Werner, J.E., Howe, S.D., 2007. An Overview of Current and Past W-UO [2] CERMET Fuel Fabrication Technology. Idaho National Lab. (INL), Idaho Falls, ID (United States).
- Burns, D., Johnson, S., 2020. Nuclear thermal propulsion reactor materials. In: Nuclear Materials. IntechOpen.
- Bushman, A., Carpenter, D.M., Ellis, T.S., Gallagher, S.P., Stawicki, M.A., 2011. The Martian Surface Reactor: An Advanced Nuclear Power Station for Manned Extraterrestrial Exploration.
- Chai, X., Guan, C., Deng, J., Zhang, T., Liu, X., 2022. Preliminary conceptual design of a moderated micro nuclear reactor core cooled by heat pipe. *Ann. Nucl. Energy* 179, 109399.
- Gibson, M.A., Oleson, S.R., Poston, D.I., McClure, P., 2017. Nasa's kilopower reactor development and the path to higher power missions. In: 2017 IEEE Aerospace Conference. IEEE, pp. 1–14.
- Gibson, M.A., Poston, D.I., McClure, P., Godfroy, T., Sanzi, J., Briggs, M.H., 2018. The kilopower reactor using stirling technology (KRUSTY) nuclear ground test results and lessons learned. In: 2018 International Energy Conversion Engineering Conference. p. 4973.
- Guo, H., Feng, K.Y., Gu, H.Y., Yao, X., Bo, L., 2021. Neutronic modeling of megawatt-class heat pipe reactors. *Ann. Nucl. Energy* 154, 108140.
- Guo, K., Zhang, Y., Lin, X., Huang, J., Wang, C., Qiu, S., Tian, W., Su, G., 2023. Transient thermoelectric characteristics of the principle prototype for the heat pipe cooled nuclear silent themoelectric reactor (NUSTER). *Ann. Nucl. Energy* 189, 109818.
- Haertling, C., Hanrahan, Jr., R.J., 2007. Literature review of thermal and radiation performance parameters for high-temperature, uranium dioxide fueled cermet materials. *J. Nucl. Mater.* 366, 317–335.
- Ingersoll, D.T., Houghton, Z.J., Bromm, R., Desportes, C., 2014. Nuscale small modular reactor for co-generation of electricity and water. *Desalination* 340, 84–93.
- Kim, K.K., Lee, W., Choi, S., Kim, H.R., Ha, J., 2014. Smart: The first licensed advanced integral reactor. *J. Energy Power Eng.* 8, 94.
- Li, S.N., Liang, Z.T., Yan, B.H., 2022. A medium temperature heat pipe cooled reactor. *Ann. Nucl. Energy* 172, 109068.
- Liu, S., She, D., Liang, J.-g., Wang, K., 2015. Development of random geometry capability in RMC code for stochastic media analysis. *Ann. Nucl. Energy* 85, 903–908.
- Liu, S., She, D., Liang, J.-g., Wang, K., 2016a. Depletion benchmarks calculation of random media using explicit modeling approach of RMC. *Ann. Nucl. Energy* 87, 167–175.
- Liu, S., Yuan, Y., Yu, J., She, D., Wang, K., 2018. On-the-fly treatment of temperature dependent cross sections in the unresolved resonance region in RMC code. *Ann. Nucl. Energy* 111, 234–241.
- Liu, S., Yuan, Y., Yu, J., Wang, K., 2016b. Development of on-the-fly temperature-dependent cross-sections treatment in RMC code. *Ann. Nucl. Energy* 94, 144–149.
- Ma, K., Hu, P., 2022. Preliminary conceptual design and neutronics analysis of a heat pipe cooled traveling wave reactor. *Ann. Nucl. Energy* 168, 108907.
- McClure, P.R., 2015. Design of megawatt power level heat pipe reactors.
- McClure, P.R., Poston, D.I., Dasari, V.R., Reid, R.S., 2015. Design of Megawatt Power Level Heat Pipe Reactors. Report of Los Alamos National Laboratory, USA.
- Powers, J.J., Wirth, B.D., 2010. A review of TRISO fuel performance models. *J. Nucl. Mater.* 405, 74–82.
- Song, D., Zeng, W., Liu, S., et al., 2014. Safety aspects of small and medium size reactor ACP100.
- Sterbentz, J.W., Werner, J.E., McKellar, M.G., Hummel, A.J., Kennedy, J.C., Wright, R.N., Biersdorff, J.M., 2017. Special Purpose Nuclear Reactor (5 MW) for Reliable Power At Remote Sites Assessment Report. Tech. Rep., Idaho National Lab. (INL), Idaho Falls, ID (United States).
- Stewart, M.E.M., 2015. A historical review of cermet fuel development and the engine performance implications. *Nucl. Emer. Technol. Space* 2015.
- Subki, H., 2020. Advances in small modular reactor technology developments.
- Sun, H., Ma, P., Liu, X., Tian, W., Qiu, S., Su, G., et al., 2018. Conceptual design and analysis of a multipurpose micro nuclear reactor power source. *Ann. Nucl. Energy* 121, 118–127.
- Swartz, M.M., Byers, W.A., Lojek, J., Blunt, R., 2021. Westinghouse evinci™ heat pipe micro reactor technology development. In: International Conference on Nuclear Engineering, vol. 85246. American Society of Mechanical Engineers, V001T04A018.
- Wang, K., Li, Z., She, D., Xu, Q., Qiu, Y., Yu, J., Sun, J., Fan, X., Yu, G., et al., 2015. RMC-a Monte Carlo code for reactor core analysis. *Ann. Nucl. Energy* 82, 121–129.
- Webb, J.A., Charit, I., 2012. Analytical determination of thermal conductivity of W-UO₂ and W-UN CERMET nuclear fuels. *J. Nucl. Mater.* 427, 87–94.
- Wu, Y., Bai, Y., Song, Y., Huang, Q., Zhao, Z., Hu, L., 2016. Development strategy and conceptual design of China lead-based research reactor. *Ann. Nucl. Energy* 87, 511–516.
- Yan, B.H., Wang, C., Li, L.G., 2020. The technology of micro heat pipe cooled reactor: A review. *Ann. Nucl. Energy* 135, 106948.
- Zhang, W., Zhang, D., Wang, C., Tian, W., Qiu, S., Su, G., 2020. Conceptual design and analysis of a megawatt power level heat pipe cooled space reactor power system. *Ann. Nucl. Energy* 144, 107576.
- Zheng, L., Huang, S., Wang, K., 2020. Criticality benchmarking of ENDF/B-VIII. 0 and JEFF-3.3 neutron data libraries with RMC code. *Nucl. Eng. Technol.* 52, 1917–1925.